Single-Blade Individual Pitch Control with Phase Compensation for Wind Turbine Periodic Blade Load Reductions

Sharma, Ayush; Hummel, Jesse I.S.; Mulders, Sebastiaan P.

DOI
10.23919/ACC63710.2025.11107742

Publication date
2025

Document Version
Final published version

Published in
Proceedings of the American Control Conference, ACC 2025

2025 American Control Conference (ACC)
July 8-10, 2025. Denver, CO, USA

Single-Blade Individual Pitch Control with Phase Compensation for Wind Turbine Periodic Blade Load Reductions

Ayush Sharma[1], Jesse I.S. Hummel[1], and Sebastiaan P. Mulders[1]

Abstract— **As wind turbine sizes and their rated power capacities increase, the spatial and temporal load imbalances over the rotor surface increase due to larger wind asymmetries, aerodynamic imbalances, and calibration offsets. The multi-blade coordinate (MBC) transform-based individual pitch control (IPC) has garnered significant attention in the literature, and it considers loads in a non-rotating reference frame. This leads to increased pitch actuation for all wind turbine blades when subject to large load imbalances. On the contrary, the single-blade control (SBC) IPC strategy is well suited for handling such load imbalances as it involves equipping each blade with a localized control system, thereby ensuring an independent operation in a rotating reference frame. However, unlike MBC transform-based IPC, the effects of system phase lag on SBC performance have not been investigated. This article investigates the effects of such phase lags and multivariable coupling on SBC performance, and proposes a novel framework for phase compensation in SBC as a convenient method for constructing and calibrating a lead compensator. Using mid-fidelity OpenFAST simulations, it is demonstrated that phase compensation in SBC improves load mitigation at the targeted frequencies and reduces actuation effort. In contrast, the absence of phase compensation can lead to load amplifications, especially for larger wind turbines.**

I. INTRODUCTION

In the previous two decades, the hub heights and rotor diameters of wind turbines have increased rapidly to capture more wind energy [1], with rotors as big as 220 m available as of 2022. As the wind turbine sizes continue to increase, the mitigation of the periodic loads is becoming increasingly important to increase its components' lives. Periodic loading exists on wind turbine blades as a consequence of different phenomena, such as wind shear, tower shadow, yaw misalignment, and turbulence, which causes fatigue damage to the rotating and stationary components of the wind turbine [2]. These periodic loads, and consequently the damage caused by them, increase with increasing rotor diameters due to an increase in the variability of wind speeds sampled by the blades.

Furthermore, as wind turbine blades continue to get larger, it is becoming increasingly necessary to construct lighter and more flexible blades to reduce material and manufacturing costs [3]. Another engineering challenge, therefore, is to retain the load-carrying capacity on such larger yet flexible blades. Active blade load control has shown promise in mitigating the periodic blade loads, thereby enabling more reliable and lighter-weight designs [4].

[1]Delft University of Technology, Delft Center for Systems and Control, Mekelweg 2, 2628 CD, Delft, The Netherlands. Email: ayushs.dtu@gmail.com, {j.i.s.hummel, s.p.mulders}@tudelft.nl

Modern wind turbines are equipped with pitch actuators – typically hydraulic or electric – which are used to pitch the blades for rotor speed control (also known as collective pitch control or CPC) and damping the tower side-side [5], [6] and fore-aft motion [7], [8]. Individual pitch control (IPC) is an active control strategy that utilizes these actuators to individually pitch the blades to distinct angles, out-of-phase with each other, to mitigate the periodic out-of-plane (OoP) blade loads [2]. As the periodic OoP loads consist of several harmonic components with frequencies concentrated mostly at integer multiples of the rotor rotational frequency (nP), common in IPC literature is to use IPC at 1P and 2P frequencies to mitigate the loads at these frequencies. As both CPC and IPC are active in different frequency ranges, common in literature is to design the two separately [9].

Among the several methods of performing IPC, the most commonly employed approach uses Multi-blade coordinate (MBC) transformation [10]. It involves projecting the OoP moments onto a non-rotating two-axis reference frame using the MBC transform before being acted upon by two 'centralized' controllers. This transformation demodulates sinusoidal load signals into DC signals, allowing for the use of classical integral (I) or proportional-integral (PI) controllers. Another strategy of performing IPC, known as Single blade control (SBC) [11], [12], employs no load transformation but acts directly on signals in the rotating reference frame. This is achieved by equipping each blade with its own controller that generates periodic pitch commands in proportion to the load experienced by that blade. However, as the input signals to the controllers are now sinusoidal or AC, I or PI controllers cannot be used, and as such, controllers in SBC take the form of bandpass filters [12], [13] centered around the targeted frequencies.

Both of these IPC strategies are effective in reducing the variation of the OoP loads, as has been proven in IPC literature using mid to high-fidelity simulations [14]. However, the manner in which load imbalances are handled differs between the two. When a wind turbine using MBC transform-based IPC is subject to load imbalances, its controllers make pitch adjustments to all blades rather than just the unbalanced blade, given that the controllers act on the projections of the resultant load on a stationary reference frame. For instance, [15] notes that aerodynamic imbalances induce 1P-frequency variations in the yaw and tilt moments, resulting in pitch action at the 2P frequency. In SBC, on the other hand, since the generated pitch command for a blade is proportional to the load experienced by only that blade, higher loads due to any asymmetric imbalances result

979-8-3315-6937-2/$31.00 ©2025 AACC

in an increased pitch actuation only for the unbalanced blade. As the load imbalances for larger wind turbines shall be higher, SBC may be better suited for IPC on such turbines as it avoids any unnecessary periodic pitch activity and, given its decentralized operating regime, may even result in potentially higher fatigue damage mitigation compared to MBC transform-based control.

However, before SBC is employed in large wind turbines, three aspects require investigation: the inter-axis coupling (multivariable coupling between pitch inputs and blade moment outputs), the effects of system phase lag, and phase compensation in SBC. The impetus for this investigation arises from MBC transform-based control, where research has revealed that system phase lag (such as due to actuator and blade dynamics) results in a coupling between the D and Q axes, and large phase lag can deteriorate performance [16], [17]. Its remedy involves including an azimuth advance in the inverse MBC transformation [17], [18]. In SBC literature, however, a diagonal control structure has always been used, and a formal investigation of the effects of phase lag on SBC performance and inter-axis coupling has not been conducted in the literature.

This article investigates the inter-axis coupling in the rotating reference frame, and proposes a novel phase compensation framework for mitigating any nP harmonic with SBC. This phase compensation is shown to improve SBC's load mitigation performance and enable higher harmonics mitigation, while also reducing the actuation effort.

The paper is organized as follows: Section II reviews the design of the conventional SBC controllers. Section III investigates the degree of inter-axis coupling in SBC and the effects of phase lag on SBC performance. Section IV presents the modified SBC framework for phase compensation, followed by its frequency domain analysis in Section V and calibration in Section VI. In the end, Section VII validates the performance of this controller through mid-fidelity OpenFAST simulations.

II. CONVENTIONAL SINGLE-BLADE CONTROL

A schematic of a typical single-blade control-based individual pitch control framework for a three-bladed wind turbine [9] is shown in Figure 1. This technique operates in the rotational reference frame since the blade loads are measured and acted upon in the rotating frame itself. The OoP moments generated by the wind turbine blades, M_i with $i \in \{1, 2, 3\}$, are measured by strain gauges located at the root of these blades. Each blade is equipped with its own controller, which acts on the OoP moment and generates a periodic individual pitch command, $\tilde{\theta}_k$ with $k \in \{1, 2, 3\}$. These commands are then added to the collective pitch command θ_0, such that the commanded pitch input to the blade actuator is

$$\theta_k = \theta_0 + \tilde{\theta}_k. \tag{1}$$

The controllers $C(s)$ that generate the individual pitch commanded in SBC take the form of variable-frequency bandpass filters in series with a proportional gain $K_{\mathrm{p},n}$. For an order of two, such a controller would utilize a bandpass filter of the form

$$H_n(s, \Omega) = \frac{2\zeta n\Omega s}{s^2 + 2\zeta n\Omega s + (n\Omega)^2}. \tag{2}$$

Here Ω is the wind turbine rotor speed, and $n \in \{1, 2, 3, ...\}$ is the targeted harmonic of the controller. Note that a variable natural frequency characteristic is required to account for a varying rotor speed, especially if SBC is used in below-rated conditions. When multiple harmonics are to be attenuated simultaneously, each controller block may consist of multiple bandpass filters connected in parallel, with each bandpass filter centered at a distinct targeted frequency and using a distinct gain.

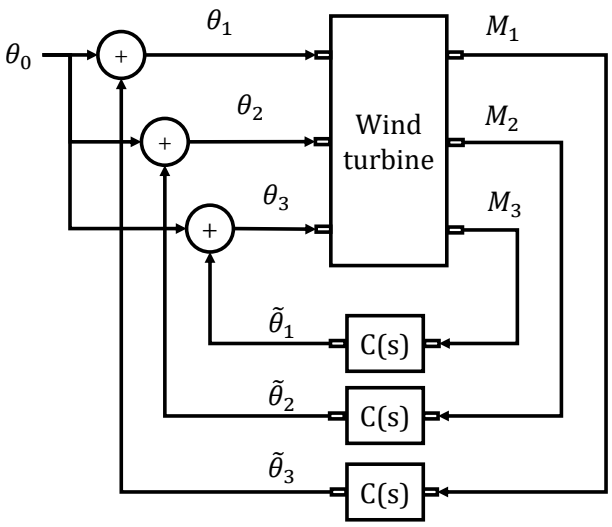

Fig. 1. Block diagram of conventional single blade control-based individual pitch control for a three-bladed wind turbine. The turbine blades experience out-of-plane moments M_i, and these load signals are input to three independent controllers $C(s)$, one for each blade. The controllers generate periodic individual pitch commands $\tilde{\theta}_k$ for the respective blade.

III. EFFECTS OF COUPLING AND PHASE LAG

This section begins with an investigation of the degree of inter-axis coupling in the rotating reference frame, followed by a study of the effects of phase lag on SBC performance.

A. Coupling Analysis

To investigate the degree of coupling in the rotating reference frame, a Relative Gain Array (RGA) [19] analysis is used. The RGA is defined as

$$R(\mathrm{j}\omega) = G_{\mathrm{p}}(\mathrm{j}\omega) \odot \left(G_{\mathrm{p}}(\mathrm{j}\omega)^{-1}\right)^{\top}, \tag{3}$$

where $\odot$ denotes an element-by-element multiplication (also known as the Hadamard or Schur product), and $G_{\mathrm{p}}(\mathrm{j}\omega)$ is the frequency response of the linearized multiple-input multiple-output (MIMO) transfer function between the wind turbine pitch inputs θ_k and OoP moments M_i, with $i, k \in \{1, 2, 3\}$, including the actuator dynamics[1].

[1]A second-order transfer function is used to model the actuator dynamics, which can be extended to include blade dynamics and dynamic inflow.

For this RGA analysis, linearizations of the IEA 15MW wind turbine [20] are obtained using OpenFAST v3.5.3 [21] at six operating points spaced evenly in the wind speed range of 7 – 25 m/s. At each operating point, 36 linearized models are obtained, evenly spaced over a full rotor rotation. The model order is set to have a total of 14 states, 3 inputs (blade pitch angles), and 3 outputs (blade root OoP moments).

At all operating points and for all azimuth positions, the calculated RGA matrix is close to identity, which indicates that the coupling between the three axes is negligible. That is, the output M_i is barely affected by an input θ_k for $i \neq k$. This result holds for any arbitrary actuator dynamics and even when the actuator dynamics on the three blades are made dissimilar. Similar results are obtained at the 2P frequency. From this, it is concluded that a diagonal controller structure can be used to develop SBC architectures, even for larger wind turbines.

B. Motivating Example – Load Mitigation Performance

In practice, there exists a phase lag between commanding a certain pitch angle and its effect being reflected on the blade loads of a wind turbine. This lag occurs because of communication delays, phase lag induced by the actuator dynamics [22], blade dynamics, and the time taken by the flow field around the blade to settle (known as dynamic inflow [23]).

This phase lag may be even more significant for longer and more flexible blades. For MBC-based IPC without any phase compensation, it is known that large phase lag may aggravate the blade load variations [18]. However, the effects of this phase lag on the load mitigation performance of SBC are yet unknown.

For this investigation, a realistic mid-fidelity simulation study is carried out using OpenFAST. The study considers a turbine without any IPC and with 1P+2P SBC. A wind profile of 20 m/s with a Kaimal IEC 61400-1 ED3 turbulence spectrum [24] is chosen. The chosen 1P+2P SBC controllers are given by (2) with $\Omega = 0.79$ rad/s and $\zeta = 0.05$, with $n = 1$ and $n = 2$ for the 1P and 2P control loops, respectively. The gains for the 1P and 2P controllers are set as $K_{\mathrm{p},1} = 5 \times 10^{-6}$ and $K_{\mathrm{p},2} = 2.5 \times 10^{-6}$, respectively. These parameters were chosen as they yielded sufficient stability margins and closed-loop load mitigation performance. The simulations are run with these configurations for a total of 3300 seconds, where the first 300 seconds of data is discarded to exclude the initialization transient effects.

Figure 2 shows the frequency-averaged power spectrum of the OoP moments that is obtained by determining a frequency-domain estimate of the plant transfer function. It is seen that the use of SBC without any phase compensation deteriorates the load mitigation performance to the point where the 2P load is amplified instead of being reduced. Figure 3 shows that this load amplification arises as a consequence of a sensitivity peak near the 2P frequency, with the sensitivity defined as

$$S(s) = (1 + L(s))^{-1}. \tag{4}$$

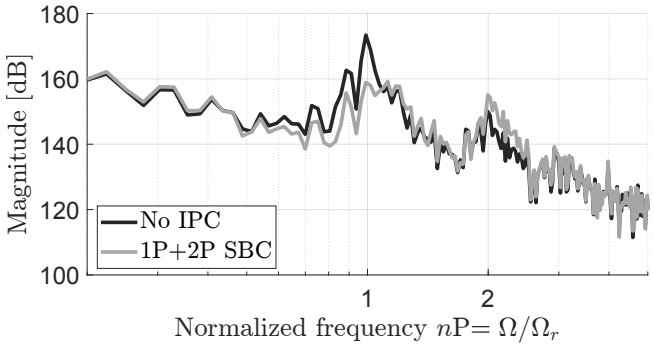

Fig. 2. Frequency averaged power spectrum of the out-of-plane plane blade moment obtained with no individual pitch control (IPC) and single-blade control (SBC) at 1P and 2P frequencies. The use of SBC without phase compensation amplifies the 2P load instead of mitigating it. This is due to uncompensated dynamics phase losses in the closed-loop system.

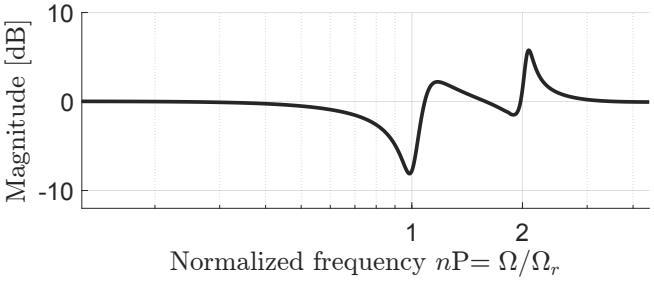

Fig. 3. Closed-loop sensitivity in the rotating frame. While attenuation at 1P frequency is possible, large system phase lag leads to insufficient phase around the 2P frequency, causing a sensitivity peak close to the 2P frequency.

Here, $L(s)$ is the open-loop transfer function from the controller input to the plant output. This sensitivity peak is due to a reduced phase margin at this frequency, and can be decreased by adding phase at this particular frequency. This phase compensation framework is discussed next.

IV. PHASE COMPENSATION FRAMEWORK

As shown, system phase lag deteriorates the single-blade control performance. Its remedy involves advancing the phase of the generated individual pitch command to compensate for the phase lag. An architecture for achieving this phase advancement in SBC is shown in Figure 4 and is indicated by the blue dashed box.

The conventional bandpass filter-based SBC controller is extended by including a first-order all-pass filter of the form

$$A_n(s) = \frac{s - n\Omega}{s + n\Omega}, \tag{5}$$

where s is the Laplace operator. This all-pass filter shifts the bandpass filtered n^{th} harmonic (with frequency $n\Omega$) by $90°$. This shifted signal is multiplied by $\sin\psi$, while the original bandpass filtered harmonic is multiplied by $\cos\psi$, where ψ is the phase advance required at the *n*P frequency. The resulting summed signal, as shown in Figure 4, is the original *n*P harmonic shifted by an angle of ψ radians. This resulting phase-compensating block is labeled as $\Pi_n(s, \psi)$,

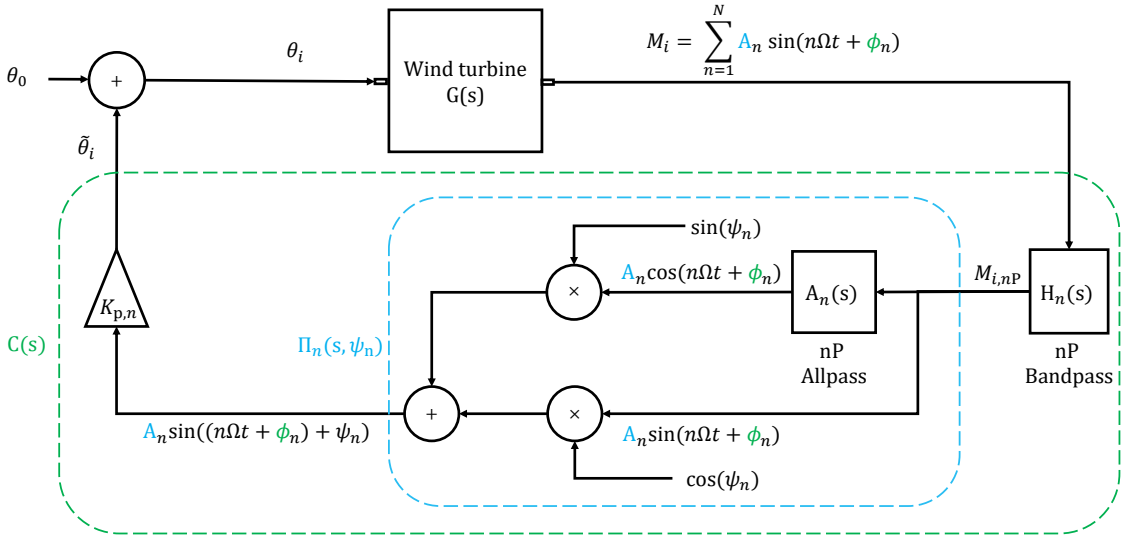

Fig. 4. Single-blade control with phase compensation (blue-dashed box) acting on the periodic load M_i for a single wind turbine blade. For phase advancement, an all-pass filter $A_n(s)$ is added, which phase shifts the bandpass filtered signal by 90°. The original and the phase-shifted signals are scaled with $\cos\psi$ and $\sin\psi$ and then summed, resulting in a signal advanced by ψ radians in phase with respect to the original n^{th} harmonic.

and its transfer function is given as

$$\Pi_n(s,\psi) = \cos(\psi) + \sin(\psi)\frac{s - n\Omega}{s + n\Omega}. \tag{6}$$

Such phase-compensating blocks may be employed in each control loop targeting a distinct OoP harmonic, allowing for different phase advances at different frequencies. A frequency domain analysis of this phase compensation framework is presented next.

V. FREQUENCY DOMAIN ANALYSIS

This section first analyzes the proposed phase compensation framework in the frequency domain, and subsequently combines it with the controller and plant transfer functions to obtain the loop-gain for analysis and controller calibration.

A. Phase Compensation Block

The transfer function of the phase compensation block given in (6) can be rearranged as

$$\Pi_n(s,\psi) = \kappa_{\text{p}} \left(\frac{\frac{s}{\Omega_{\text{d}}} + 1}{\frac{s}{\Omega_{\text{t}}} + 1} \right), \tag{7}$$

with,

$$\kappa_{\text{p}} = \cos(\psi) - \sin(\psi),$$
$$\Omega_{\text{d}} = \frac{\cos(\psi) - \sin(\psi)}{\cos(\psi) + \sin(\psi)} n\Omega,$$
$$\Omega_{\text{t}} = n\Omega.$$

This representation reveals that the phase compensation block functions as a special type of lead or lag compensator, depending on the specified phase angle ψ. Also, depending on the amount of phase advance specified, the compensator may be non-minimum phase as it may introduce a right-half plane (RHP) zero. Figure 5 shows the frequency responses of phase compensator blocks that phase advance the 1P frequency component by $40°$, $60°$, and $80°$.

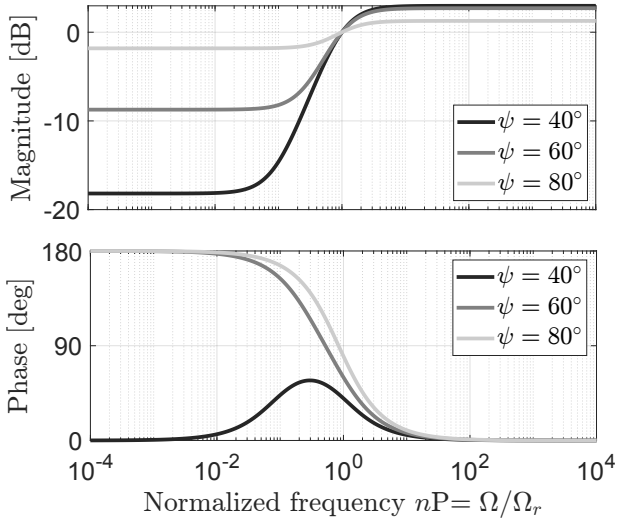

Fig. 5. Frequency responses of the phase compensator block $\Pi(s,\psi)$ for different phase angles. This block functions as a special kind of lead compensator that does not affect the gain at the target frequency but adds the required amount of phase at it. For the phases of $60°$ and $80°$ this compensator is non-minimum phase.

The frequency response of this compensator is different from those of typical lead compensators in two ways. Firstly, the proposed compensator has a unity gain at the target frequency, while a lead compensator always provides amplification at the target frequency. Secondly, the proposed compensator may add a phase of $180°$ at low frequencies if it is non-minimum phase, while a lead compensator always adds zero phase at low frequencies.

B. Open-loop Transfer Function

For minimizing the 1P and the 2P out-of-plane (OoP) moment amplitudes with the proposed phase-advancing con-

troller architecture, the single-input single-output (SISO) open-loop transfer function relating the blade moment (output) to the pitch (input) is derived as

$$L_{ik}(s) = -G_{ik}(s) \cdot [K_{\mathrm{p},1}\Pi_1(s,\psi_1)H_1(s) + K_{\mathrm{p},2}\Pi_2(s,\psi_2)H_2(s)\ ]. \tag{8}$$

Here, $G_{ik}(s) = G_{\mathrm{p},ik}(s)G_{\mathrm{a}}(s)$, with $G_{\mathrm{p},ik}(s)$ as the linearized plant transfer function from the k^{th} pitch angle to the i^{th} moment, and $G_{\mathrm{a}}(s)$ as the actuator dynamics. From (8), it can be seen that despite having two controllers (1P and 2P) per blade, the open-loop gain is a single SISO transfer function, implying that a single transfer function given can be used to tune several controllers simultaneously for SBC. The next section discusses the use of (8) for tuning the single-blade controller and presents an example for a specific operating point.

VI. CONTROLLER TUNING

The phase compensating 1P and 2P controllers can be tuned using (8) for the operating point of linearization, by observing the Nyquist plots and closed-loop sensitivity plots. Different tunings can be obtained for different operating points, and then gain scheduling can be used to ensure optimal performance and stability across different wind speeds. However, the frequency response of the plant transfer function $G_{\mathrm{p},ik}(s)$ also varies with the rotor azimuth of linearization. This implies that a controller tuning chosen to yield certain stability margins for a given rotor azimuth may be suboptimal or even unstable for other rotor azimuth angles. This limitation is addressed by using the plant linearization that yields the smallest stability margins across all rotor azimuths in (8). Tuning a controller to have sufficient stability margins for this azimuth results in a conservative tuning and stable closed-loop behavior for all other azimuth positions for the given system.

As an illustrative example and for later simulations, a controller is now tuned for an operating point of 20 m/s wind speed, for which certain considerations are first made. Firstly, the transfer function at a rotor azimuth of 150° is used, as it yields the least stability margins. Secondly, pitch actuator dynamics $G_{\mathrm{a}}(s)$ are modeled as a harmonic oscillator with a natural frequency of $\omega_{\mathrm{a}} = 2$ rad/s and a damping of $\zeta = 1/\sqrt{2}$, and it is assumed that all three blade actuators share the same dynamics. Lastly, the chosen bandpass filters are described by (2), while the chosen phase compensators are described by (6), with $n = 1$ and $n = 2$ for the 1P and 2P control loops, respectively. Note that both the bandpass filters use the Q-factor $\mathrm{Q} = 10$, and therefore $\zeta = 1/(2\mathrm{Q}) = 0.05$.

The next step in the tuning process is to specify the phase advance values ψ_1 and ψ_2. As the objective of phase advance is to compensate for the phase lag in the system, the phase advance values are chosen as the phase lag of the chosen transfer function $-G_{ik}(s)$ at the 1P and the 2P frequencies, which are $\psi_1 = 53.11^\circ$ and $\psi_2 = 114.62^\circ$, respectively.

The final step involves tuning the proportional gains $K_{\mathrm{p},1}$ and $K_{\mathrm{p},2}$, the selection of which actually involves a trade-off: using higher proportional gains results in higher attenuation at 1P and 2P frequencies at the expense of reduced stability margins and increased sensitivity at other frequencies due to the waterbed effect [19]. The gains $K_{\mathrm{p},1} = K_{\mathrm{p},2} = 7.5 \times 10^{-6}$ are chosen, and are seen to well achieve this compromise, achieving a minimum gain margin of 7.5 dB and a phase margin of 82.5°.

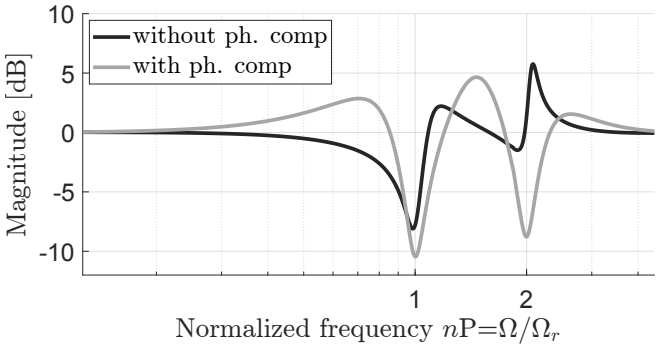

Fig. 6. Closed-loop sensitivity in the rotating frame for non-phase compensating and phase compensating SBC controllers. The use of phase compensation enables attenuation at the 2P frequency and the use of higher proportional gains, which increases the attenuation at 1P and 2P frequencies.

Figure 6 shows the rotating-frame sensitivity for the tuned phase compensating controller and compares it with an untuned non-phase compensating configuration. It can be seen that the use of phase compensation enables attenuation at the 2P frequency, and higher proportional gains allow for higher attenuation at 1P and 2P frequencies.

VII. RESULTS AND DISCUSSION

To verify the efficacy of phase compensation and the presented frequency domain analysis, mid-fidelity OpenFAST simulations are performed using the same setup as described in Section III-B.

Figure 7 shows the frequency averaged power spectrum for one of the OoP moments for different simulation cases. It is observed that performing 1P+2P SBC with phase compensation and controller tuning not only attenuates the 1P peak more effectively but also achieves a near elimination of the 2P peak. This result is in accordance with the SISO sensitivity analysis of Figure 6.

Another benefit of phase compensation is that it reduces the required pitch activity. This result can be verified by evaluating the actuator duty cycle (ADC) [25], defined as

$$\mathrm{ADC} = \frac{1}{T}\int_0^T \frac{\dot{\beta}(t)}{\dot{\beta}_{\max}} dt. \tag{9}$$

Here $\dot{\beta}(t)$ is the pitch rate of the blade, $\dot{\beta}_{\max}$ is the maximum allowable pitch rate, and T is the time duration over which the ADC is calculated. With phase compensation, SBC achieves a 27 $\%$ percent lesser ADC compared to the non-phase compensating case.

This reduction in pitch activity is due to a reduction in the controller sensitivity because of phase compensation. The controller sensitivity function from the pitch input to the

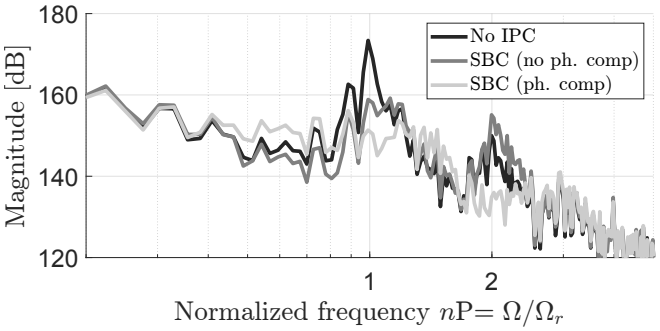

Fig. 7. Frequency averaged power spectrum of the out-of-plane moment. Performing 1P + 2P IPC with phase lag compensation allows for increased attenuation at 1P and eliminates the 2P peak.

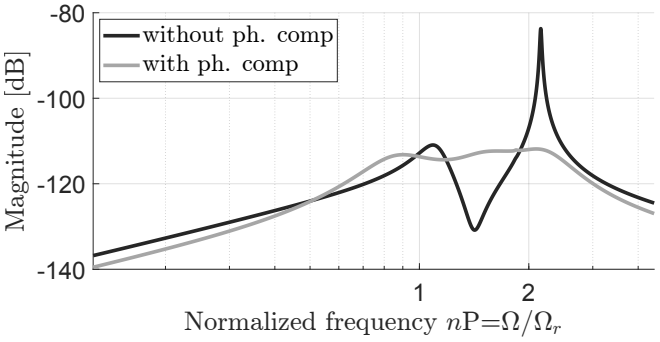

Fig. 8. Closed-loop controller sensitivity in the rotating reference frame. Phase compensation significantly reduces the controller sensitivity around the 2P frequency, which leads to a remarkable reduction in the pitch activity compared to the non-phase compensating case.

blade moment is given as

$$KS(s) = \frac{C(s)}{1 + L(s)}. \tag{10}$$

Figure 8 shows that phase compensation significantly reduces the controller-sensitivity peak close to the 2P frequency, which leads to lesser 2P pitch activity and, therefore, yields significantly less ADC.

VIII. CONCLUSIONS

The analysis in this paper shows that the system dynamics in the rotating reference frame can be considered as a diagonal system as a consequence of negligible inter-axis coupling. However, system phase lag can lead to load amplification at higher harmonics if not accounted for in the IPC strategy. A novel and convenient phase compensation architecture has been proposed for the SBC framework, resulting in a special type of lead compensator. Mid-fidelity OpenFAST simulation results verify that with phase compensation, SBC achieves higher load mitigation at reduced actuator usage. Thus, it can be concluded that phase compensation not only enables the attenuation of higher harmonics with SBC but also achieves a better load mitigation performance at reduced pitch actuation.

Future research will focus on comparing the load mitigation performance and actuator usage between MBC transform-based control and phase-compensating SBC for large-scale wind turbines.

REFERENCES

[1] Office of Energy Efficiency & Renewable Energy , "Wind Turbines: the Bigger, the Better ," 2023.

[2] E. A. Bossanyi, "Individual blade pitch control for load reduction," *Wind Energy*, 2003.

[3] X. Zhu, J. Chen, X. Shen, and Z. Du, "Impact of blade flexibility on wind turbine loads and pitch settings," *Journal of Solar Energy Engineering*, 2019.

[4] P. Veers, K. Dykes, S. Basu, A. Bianchini, A. Clifton, P. Green, H. Holttinen, L. Kitzing, B. Kosovic, J. K. Lundquist, *et al.*, "Grand challenges: wind energy research needs for a global energy transition," *Wind Energy Science*, 2022.

[5] A. K. Pamososuryo, S. P. Mulders, R. Ferrari, and J. W. van Wingerden, "On the Analysis and Synthesis of Wind Turbine Side–Side Tower Load Control via Demodulation," *Transactions on Control Systems Technology*, 2024.

[6] S. P. Mulders, T. G. Hovgaard, J. D. Grunnet, and J. W. van Wingerden, "Preventing wind turbine tower natural frequency excitation with a quasi-LPV model predictive control scheme," *Wind Energy*, 2020.

[7] E. Bossanyi, "Wind turbine control for load reduction," *Wind Energy*, 2003.

[8] J. H. Laks, L. Y. Pao, and A. D. Wright, "Control of wind turbines: Past, present, and future," in *American Control Conference (ACC)*. IEEE, 2009.

[9] W. H. A. Lio, *Blade-pitch control for wind turbine load reductions*. Springer, 2018.

[10] G. Bir, "Multi-blade coordinate transformation and its application to wind turbine analysis," in *46th AIAA Aerospace Sciences Meeting and Exhibit*, 2008.

[11] W. Leithead, V. Neilson, and S. Dominguez, "Alleviation of unbalanced rotor loads by single blade controllers," in *European Wind Energy Conference & Exhibition (EWEC)*. Curran Associates, 2009.

[12] W. Leithead, V. Neilson, S. Dominguez, and A. Dutka, "A novel approach to structural load control using intelligent actuators," in *17th Mediterranean Conference on Control and Automation*. IEEE, 2009.

[13] E. Van Solingen and J. W. van Wingerden, "Linear individual pitch control design for two-bladed wind turbines," *Wind Energy*, 2015.

[14] C. Plumley, W. Leithead, P. Jamieson, E. Bossanyi, and M. Graham, "Comparison of individual pitch and smart rotor control strategies for load reduction," in *Journal of Physics: Conference Series*. IOP Publishing, 2014.

[15] S. Kanev and T. van Engelen, "Exploring the limits in individual pitch control," in *European Wind Energy Conference (EWEC)*, 2009.

[16] V. Petrović, M. Jelavić, and M. Baotić, "Advanced control algorithms for reduction of wind turbine structural loads," *Renewable Energy*, 2015.

[17] S. P. Mulders, A. K. Pamososuryo, G. E. Disario, and J. W. van Wingerden, "Analysis and optimal individual pitch control decoupling by inclusion of an azimuth offset in the multiblade coordinate transformation," *Wind Energy*, 2019.

[18] S. P. Mulders and J. W. van Wingerden, "On the importance of the azimuth offset in a combined 1P and 2P SISO IPC implementation for wind turbine fatigue load reductions," in *American Control Conference (ACC)*. IEEE, 2019.

[19] S. Skogestad and I. Postlethwaite, *Multivariable feedback control: analysis and design*. John Wiley & Sons, 2005.

[20] E. Gaertner, J. Rinker, L. Sethuraman, F. Zahle, B. Anderson, G. Barter, N. Abbas, F. Meng, P. Bortolotti, W. Skrzypinski, *et al.*, "Definition of the IEA 15-MW offshore reference wind turbine," 2020.

[21] National Renewable Energy Laboratory (NREL), "OpenFAST v3.5.3," 2024. [Online]. Available: https://doi.org/10.5281/zenodo.10962897

[22] M. Shan, J. Jacobsen, and S. Adelt, "Field testing and practical aspects of load reducing pitch control systems for a 5 MW offshore wind turbine," in *Annual Conference and Exhibition of European Wind Energy Association*, 2013.

[23] T. Knudsen and T. Bak, "Simple model for describing and estimating wind turbine dynamic inflow," in *American Control Conference (ACC)*. IEEE, 2013.

[24] B. Jonkman, "TurbSim user's guide v2.00.00," *National Renewable Energy Laboratory (NREL)*, 2014.

[25] C. L. Bottasso, F. Campagnolo, A. Croce, and C. Tibaldi, "Optimization-based study of bend–twist coupled rotor blades for passive and integrated passive/active load alleviation," *Wind Energy*, 2013.